Rao tests for distributed target detection in interference and noise

Weijian Liu [a,b,*], Jun Liu [c], Lei Huang [d], Dujian Zou [e], Yongliang Wang [b]

[a] College of Electronic Science and Engineering, National University of Defense Technology, Changsha 410073, China
[b] Wuhan Radar Academy, Wuhan 430019, China
[c] National Laboratory of Radar Signal Processing, Xidian University, Xi'an 710071, China
[d] College of Information Engineering, Shenzhen University, Shenzhen 518055, China
[e] Graduate School at Shenzhen, Tsinghua University, Shenzhen 518060, China

ARTICLE INFO

ABSTRACT

This paper deals with the problem of detecting a distributed target in interference and noise. The target signal and interference are assumed to lie in two linearly independent subspaces, and their coordinates are unknown. The noise is Gaussian distributed, with an unknown covariance matrix. To estimate the covariance matrix, a set of training data is supposed available. We derive the Rao test and its two-step variant both in homogeneous and partially homogeneous environments. All of the proposed detectors exhibit a desirable constant false alarm rate. Numerical examples show that the proposed detectors can provide better detection performance than their natural counterparts in some scenarios.

© 2015 Elsevier B.V. All rights reserved.

1. Introduction

Detection of a distributed target in unknown disturbance is an interesting research topic. Up to now a large number of approaches have been proposed to solve the problem in various scenarios. Particularly, in [1] a distributed target is embedded in unknown Gaussian noise, and the echoes reflected by the distributed target are assumed to have the same direction. To estimate the unknown covariance matrix, a set of signal-free training (secondary) data is required. When the test (primary) data and secondary data have the identical covariance matrix, it is usually referred to as the homogeneous environment (HE) [1]. In contrast, when the primary and secondary data share the same structure of the covariance

matrix, but with unknown power mismatch, it is denoted as the partial HE (PHE) [1]. Based on the generalized likelihood ratio test (GLRT) criterion, several detectors for the HE and PHE are proposed in [1]. The Rao and Wald tests are derived in [2] for the HE and in [3] for the PHE. Remarkably, a milestone in the area of multichannel signal detection in unknown Gaussian noise is the report in [4], where the model is very general and the GLRT-based detectors are proposed and detailed analyzed. More recently, the detection model in [4] is further generalized in [5,6] and many detectors are devised. Some other related work is exploited in [7–14] and the references therein.

It is worth noting that interference is not taken into account in the references mentioned above. However, in many practical applications there usually exists interference due to electronic countermeasure (ECM) systems or civil broadcasting systems. The detection problem is addressed in [15–20] in the presence of deterministic interference under the assumption of white Gaussian

---

* Corresponding author. Tel. +86 2785965760.
E-mail addresses: liuvjian@163.com (W. Liu),
junliu@xidian.edu.cn (J. Liu), dr.lei.huang@ieee.org (L. Huang),
zoudujian@163.com (D. Zou), ylwangkjld@163.com (Y. Wang).

noise or colored Gaussian noise with known covariance matrix. Moreover, the GLRT is derived in [21] for detecting a point-like target in undernulled noise-like interference and unknown Gaussian noise. The resulting GLRT is shown to be equivalent to the adaptive coherence estimator (ACE). In [22], the problem of detecting a point-like target in deterministic interference and unknown Gaussian noise is dealt with. The interference lies in the primary and secondary data, and it is confined to a known subspace. The detection problem is solved by the method of sieves. For the distributed target detection, in [23] the echo signals reflected from the target are all assumed to come from the same direction, and the signal steering vector lies in a known subspace with an unknown coordinate. The GLRT and two-step GLRT (2S-GLRT) are proposed in the presence of deterministic interference for the HE. The detection problem in [23] is extended in [24], where the deterministic interference is assumed to lie in an unknown subspace except for the knowledge of the interference subspace dimension. Additionally, in [25] the interference and target signal are assumed to lie in two linearly independent subspaces, and the GLRT and 2S-GLRT are proposed for the HE and PHE.

Note that there exists no uniformly most powerful (UMP) test for the detection problem in [25], since the noise covariance matrix and the coordinates of the signal and interference are unknown. Hence, it may be reasonable to adopt approaches different from the GLRT and 2S-GLRT employed therein to devise detectors. Besides the GLRT criterion, the other two criteria widely used for detector design are the Rao test and Wald test, e.g., [26–30]. In this paper we adopt the Rao test, including the one-step and two-step versions, to design detectors for the detection problem in [25], since the Rao test can achieve best detection performance in some scenarios[1]. It is shown that all the proposed detectors are constant false alarm rate (CFAR) with respect to (w.r.t.) the unknown covariance matrix. Moreover, the proposed detectors can achieve better detection performance than the existing ones in some situations.

The rest of the paper is organized as follows. Section 2 formulates the detection problem to be solved. Section 3 derives the one-step Rao test and two-step Rao (2S-Rao) test in the HE and PHE. Section 4 compares the detection performance of the proposed detectors with the existing ones by Monte Carlo simulations. Finally, some concluding remarks are given in Section 5.

Notations: Matrices, vectors, scalars, are denoted by bold-face upper case letters, bold-face lower case letters, and light-face lower case letters, respectively. The superscripts $(\cdot)^*$, $(\cdot)^T$, and $(\cdot)^H$ stands for the conjugate, transpose, and conjugate transpose of a vector or matrix, respectively. The notation $\otimes$ is the Kronecker product. For a complex number a, $abs(a)$ stands for its modulus. For an $N \times K$ matrix A, $E[A]$ denotes the statistical expectation of A, $vec(A)$ vectorizes A by stacking its columns, P_A is the

orthogonal projector (projection matrix) onto the subspace spanned by the columns of A, i.e., $P_A = A(A^H A)^{-1}A^H$, and $P_A^\perp = I_N - P_A$. When A becomes a square matrix, $|A|$ and $tr(A)$ denote its determinant and trace, respectively. Further, when A turns into a positive definite matrix, $A^{1/2}$ denotes its square-root matrix (positive definite and satisfying $A^{1/2}A^{1/2} = A$), and $A^{-1/2}$ is the inverse of $A^{1/2}$. $\min(a,b)$ denotes the minimum value of a and b. $\ln f$ stands for the natural logarithm of the scalar function f, and $\partial f / \partial \Xi$ is the partial derivative of f w.r.t. Ξ, with Ξ being a vector or matrix. Moreover, $\hat{\Xi}_i$ is the maximum likelihood estimate (MLE) of Ξ under hypothesis H_i, $i = 0, 1$. Finally, I_N is an $N \times N$ identity matrix and $\mathbf{0}_{p \times q}$ is a $p \times q$ null matrix.

2. Problem formulation

Consider a radar system with N antenna elements. The target, if present, occupies K successive range cells. Denote the data in the kth range cell as an $N \times 1$ column vector x_k, $k = 1, 2, \ldots, K$. We try to make a decision between hypothesis H_0 that x_k only contains disturbance d_k and hypothesis H_1 that x_k contains disturbance d_k and useful signal s_k. The disturbance d_k consists of colored noise n_k, usually including clutter as well as thermal noise, and interference i_k. The signal s_k and interference i_k are both assumed to be deterministic and lie in two linearly independent subspaces [25]. In other words, s_k and i_k can be represented by $s_k = Hp_k$ and $i_k = Jq_k$, respectively. The $N \times p$ matrix H and $N \times q$ matrix J are both of full column rank. The columns of H spans the subspace where the signal lies, while the columns of J spans the subspace which the interference belongs to. The $p \times 1$ vector p_k is the coordinate vector for the signal, and the $q \times 1$ vector q_k is the coordinate vector for the interference. Note that the augmented matrix $B = [H, J]$ is full-column-rank due to the linear independence of the subspaces spanned by the columns of H and J, and hence $p + q \leq N$ [15–17,19,23,25]. Moreover, n_k, $k = 1, 2, \ldots, K$, is independent and identically distributed (IID), mean-zero, complex circular Gaussian vector, with a covariance matrix R_t, which is positive definitive and unknown. To estimate R_t, it is often assumed that a set of secondary data, denoted by an $N \times L$ matrix X_L, is available. These secondary data are usually collected in the vicinity of the primary data X. Let the lth column of X_L be $x_{e,l}$, $l = 1, 2, \ldots, L$, which is IID and has the covariance matrix R. In the HE $R_t = R$ [32], while in the PHE $R_t = \sigma^2 R$ [1], with σ^2 being a scaling factor accounting for unknown power mismatch between the primary and secondary data [1].

With the assumption above, the detection problem can be formulated as the following binary hypothesis test

$$\begin{cases} H_0 : X = JQ + N, X_L = N_L, \\ H_1 : X = HP + JQ + N, X_L = N_L, \end{cases} \tag{1}$$

where $P = [p_1, p_2, \ldots, p_K]$ and $Q = [q_1, q_2, \ldots, q_K]$ are the unknown coordinate matrices of the signal and interference, respectively. Note that the subspace model in (1) is very general. It either accounts for the multiple targets and/or interferences [33] or corresponds to the

---

[1] For example, the so-called modified two-step GLRT (M2S-GLRT) in [31], which essentially can be derived according to the Rao test [8], has the best detection performance in some situations.

uncertainty in the steering vector for the target and/or interference [34]. Moreover, the subspace interference model in (1) is a common assumption, widely used in the literature [15–20,22,23,25]. The justification is that in practice this information can be obtained by operating the radar in receive-only mode before the start of transmission [35].

3. The proposed detectors

In this section we develop the Rao test, as well as its two-step variation, for the detection problem in (1) both in the HE and PHE. Let $\boldsymbol{\Theta}$ be a parameter vector, partitioned as

$$\boldsymbol{\Theta} = [\boldsymbol{\Theta}_r^T, \boldsymbol{\Theta}_s^T]^T \tag{2}$$

where $\boldsymbol{\Theta}_r = vec(\boldsymbol{P})$ and $\boldsymbol{\Theta}_s = [vec^T(\boldsymbol{Q}), vec^T(\boldsymbol{R})]^T$ (in the HE) or $\boldsymbol{\Theta}_s = [\sigma^2, vec^T(\boldsymbol{Q}), vec^T(\boldsymbol{R})]^T$ (in the PHE). The $\boldsymbol{\Theta}_r$ and $\boldsymbol{\Theta}_s$ are usually called the relative and nuisance parameters, respectively. The Fisher information matrix (FIM) w.r.t. $\boldsymbol{\Theta}$ is given by [36]

$$\boldsymbol{I}(\boldsymbol{\Theta}) = E\{[\partial \ln f_1(\boldsymbol{X}, \boldsymbol{X}_L)/\partial \boldsymbol{\Theta}^*][\partial \ln f_1(\boldsymbol{X}, \boldsymbol{X}_L)/\partial \boldsymbol{\Theta}^T]\}, \tag{3}$$

where $f_1(\boldsymbol{X}, \boldsymbol{X}_L)$ is the joint probability density function (PDF) of $\boldsymbol{X}$ and $\boldsymbol{X}_L$ under H_1. For convenience, the $\boldsymbol{I}(\boldsymbol{\Theta})$ is often partitioned in the following manner:

$$\boldsymbol{I}(\boldsymbol{\Theta}) = \begin{bmatrix} \boldsymbol{I}_{\boldsymbol{\Theta}_r, \boldsymbol{\Theta}_r}(\boldsymbol{\Theta}) & \boldsymbol{I}_{\boldsymbol{\Theta}_r, \boldsymbol{\Theta}_s}(\boldsymbol{\Theta}) \\ \boldsymbol{I}_{\boldsymbol{\Theta}_s, \boldsymbol{\Theta}_r}(\boldsymbol{\Theta}) & \boldsymbol{I}_{\boldsymbol{\Theta}_s, \boldsymbol{\Theta}_s}(\boldsymbol{\Theta}) \end{bmatrix}. \tag{4}$$

It follows from [36] that the Rao test is

$$t_{Rao} = \frac{\partial \ln f_1(\boldsymbol{X}, \boldsymbol{X}_L)}{\partial \boldsymbol{\Theta}_r}\bigg|_{\boldsymbol{\Theta} = \hat{\boldsymbol{\Theta}}_0}^H [\boldsymbol{I}^{-1}(\hat{\boldsymbol{\Theta}}_0)]_{\boldsymbol{\Theta}_r, \boldsymbol{\Theta}_r} \frac{\partial \ln f_1(\boldsymbol{X}, \boldsymbol{X}_L)}{\partial \boldsymbol{\Theta}_r}\bigg|_{\boldsymbol{\Theta} = \hat{\boldsymbol{\Theta}}_0}, \tag{5}$$

where $[\boldsymbol{I}^{-1}(\hat{\boldsymbol{\Theta}}_0)]_{\boldsymbol{\Theta}_r, \boldsymbol{\Theta}_r}$ is

$$[\boldsymbol{I}^{-1}(\boldsymbol{\Theta})]_{\boldsymbol{\Theta}_r, \boldsymbol{\Theta}_r} = [\boldsymbol{I}_{\boldsymbol{\Theta}_r, \boldsymbol{\Theta}_r}(\boldsymbol{\Theta}) - \boldsymbol{I}_{\boldsymbol{\Theta}_r, \boldsymbol{\Theta}_s}(\boldsymbol{\Theta})\boldsymbol{I}_{\boldsymbol{\Theta}_s, \boldsymbol{\Theta}_s}^{-1}(\boldsymbol{\Theta})\boldsymbol{I}_{\boldsymbol{\Theta}_s, \boldsymbol{\Theta}_r}(\boldsymbol{\Theta})]^{-1} \tag{6}$$

evaluated at $\hat{\boldsymbol{\Theta}}_0$, i.e., the MLE of $\boldsymbol{\Theta}$ under H_0.

To derive the Rao test, we need the joint PDF $f_1(\boldsymbol{X}, \boldsymbol{X}_L)$, which is

$$f_1(\boldsymbol{X}, \boldsymbol{X}_L) = [\pi^{N(L+K)}\sigma^{2NK}|\boldsymbol{R}|^{L+K}]^{-1}\exp\Big\{-tr(\boldsymbol{R}^{-1}\boldsymbol{S}) - tr[\boldsymbol{R}^{-1}(\boldsymbol{X}-\boldsymbol{BD})(\boldsymbol{X}-\boldsymbol{BD})^H]/\sigma^2\Big\}, \tag{7}$$

where $\boldsymbol{S}$ is the sample covariance matrix (SCM) given by $\boldsymbol{S} = \boldsymbol{X}_L\boldsymbol{X}_L^H$, $\boldsymbol{B} = [\boldsymbol{H}, \boldsymbol{J}]$, and $\boldsymbol{D} = [\boldsymbol{P}^H, \boldsymbol{Q}^H]^H$. Taking the derivative of the logarithm of (7) w.r.t. $\boldsymbol{P}$ and $\boldsymbol{P}^*$ results in

$$\partial \ln f_1(\boldsymbol{X}, \boldsymbol{X}_L)/\partial vec(\boldsymbol{P}) = vec\Big\{[(\boldsymbol{X}-\boldsymbol{BD})^H\boldsymbol{R}_t^{-1}\boldsymbol{H}]^T\Big\} \tag{8}$$

and

$$\partial \ln f_1(\boldsymbol{X}, \boldsymbol{X}_L)/\partial vec(\boldsymbol{P}^*) = vec[\boldsymbol{H}^H\boldsymbol{R}_t^{-1}(\boldsymbol{X}-\boldsymbol{BD})], \tag{9}$$

respectively. Letting $\boldsymbol{Z} = \boldsymbol{X} - \boldsymbol{BD}$, then plugging (8) and (9) into (3) yields

$$\boldsymbol{I}_{\boldsymbol{\Theta}_r, \boldsymbol{\Theta}_r}(\boldsymbol{\Theta}) = E\Big[vec(\boldsymbol{H}^H\boldsymbol{R}_t^{-1}\boldsymbol{Z})vec^T(\boldsymbol{H}^T\boldsymbol{R}_t^{-T}\boldsymbol{Z}^*)\Big]$$
$$= E\Big\{\Big[\boldsymbol{I}_K \otimes \boldsymbol{H}^H\boldsymbol{R}_t^{-1}\Big]vec(\boldsymbol{Z})\Big[(\boldsymbol{I}_K \otimes \boldsymbol{H}^T\boldsymbol{R}_t^{-T})vec(\boldsymbol{Z}^*)\Big]^T\Big\}$$

$$= \Big[\boldsymbol{I}_K \otimes \boldsymbol{H}^H\boldsymbol{R}_t^{-1}\Big]E\big[vec(\boldsymbol{Z})vec^H(\boldsymbol{Z})\big]\Big[\boldsymbol{I}_K \otimes \boldsymbol{R}_t^{-1}\boldsymbol{H}\Big]$$
$$= \Big[\boldsymbol{I}_K \otimes \boldsymbol{H}^H\boldsymbol{R}_t^{-1}\Big][\boldsymbol{I}_K \otimes \boldsymbol{R}_t]\Big[\boldsymbol{I}_K \otimes \boldsymbol{R}_t^{-1}\boldsymbol{H}\Big]$$
$$= \boldsymbol{I}_K \otimes \boldsymbol{H}^H\boldsymbol{R}_t^{-1}\boldsymbol{H}, \tag{10}$$

where we have used $vec(\boldsymbol{A}_1\boldsymbol{A}_2\boldsymbol{A}_3) = (\boldsymbol{A}_3^T \otimes \boldsymbol{A}_1)vec(\boldsymbol{A}_2)$ ([37], p. 35), $E[vec(\boldsymbol{Z})vec^H(\boldsymbol{Z})] = \boldsymbol{I}_K \otimes \boldsymbol{R}_t$, and $(\boldsymbol{A}_4 \otimes \boldsymbol{A}_5)(\boldsymbol{A}_6 \otimes \boldsymbol{A}_7) = \boldsymbol{A}_4\boldsymbol{A}_6 \otimes \boldsymbol{A}_5\boldsymbol{A}_7$ ([37], p. 32) in the second, fourth, and last equalities, respectively. $\boldsymbol{A}_i$, $i = 1, 2, \ldots, 7$, in the equalities above is an arbitrary conformable matrix.

Note that $\boldsymbol{I}_{\boldsymbol{\Theta}_r, \boldsymbol{\Theta}_s}(\boldsymbol{\Theta})$ is a null matrix. Hence, from (6) we have

$$[\boldsymbol{I}^{-1}(\boldsymbol{\Theta})]_{\boldsymbol{\Theta}_r, \boldsymbol{\Theta}_r} = \boldsymbol{I}_{\boldsymbol{\Theta}_r, \boldsymbol{\Theta}_r}^{-1}(\boldsymbol{\Theta}) = (\boldsymbol{I}_K \otimes \boldsymbol{H}^H\boldsymbol{R}_t^{-1}\boldsymbol{H})^{-1}. \tag{11}$$

Substituting (8) and (11) into (5) and setting $\boldsymbol{P} = \boldsymbol{0}_{p \times K}$ leads to the Rao test for given $\boldsymbol{Q}$ and $\boldsymbol{R}_t$

$$t_{Rao|Q, \boldsymbol{R}_t} = vec\Big\{\big[(\boldsymbol{X}-\boldsymbol{JQ})^H\boldsymbol{R}_t^{-1}\boldsymbol{H}\big]^T\Big\}\Big[\boldsymbol{I}_K \otimes (\boldsymbol{H}^H\boldsymbol{R}_t^{-1}\boldsymbol{H})^{-1}\Big]$$
$$\times vec\Big[\boldsymbol{H}^H\boldsymbol{R}_t^{-1}(\boldsymbol{X}-\boldsymbol{JQ})\Big]$$
$$= vec\Big\{\big[(\boldsymbol{X}-\boldsymbol{JQ})^H\boldsymbol{R}_t^{-1}\boldsymbol{H}\big]^T\Big\}vec\big[(\boldsymbol{H}^H\boldsymbol{R}_t^{-1}\boldsymbol{H})^{-1}\boldsymbol{H}^H\boldsymbol{R}_t^{-1}(\boldsymbol{X}-\boldsymbol{JQ})\big]$$
$$= tr\Big[(\boldsymbol{X}-\boldsymbol{JQ})^H\boldsymbol{R}_t^{-1}\boldsymbol{H}(\boldsymbol{H}^H\boldsymbol{R}_t^{-1}\boldsymbol{H})^{-1}\boldsymbol{H}^H\boldsymbol{R}_t^{-1}(\boldsymbol{X}-\boldsymbol{JQ})\Big]. \tag{12}$$

3.1. One-step Rao test

In order to obtain the explicit one-step Rao test, we need the MLEs of $\boldsymbol{Q}$, $\boldsymbol{R}$, and σ^2 under H_0. In light of (7), the MLE of $\boldsymbol{R}$ under H_0 for given $\boldsymbol{Q}$ is

$$\hat{\boldsymbol{R}}_0 = \Big[\boldsymbol{S} + (\boldsymbol{X}-\boldsymbol{JQ})(\boldsymbol{X}-\boldsymbol{JQ})^H/\sigma^2\Big]/(K+L). \tag{13}$$

Inserting (13) into (7) results in

$$f_0(\boldsymbol{X}, \boldsymbol{X}_L; \hat{\boldsymbol{R}}_0) = [(L+K)/(e\pi)]^{N(K+L)}|\boldsymbol{S}|^{-(L+K)}\big[\sigma^{2NK}|\boldsymbol{I}_K + (\boldsymbol{X}-\boldsymbol{JQ})^H\boldsymbol{S}^{-1}(\boldsymbol{X}-\boldsymbol{JQ})/\sigma^2\big|^{L+K}\big]^{-1}, \tag{14}$$

where we have used the identity (A1-2) in [4], i.e.,

$$|\boldsymbol{C}_1 + \boldsymbol{C}_2\boldsymbol{C}_3\boldsymbol{C}_4| = |\boldsymbol{C}_1||\boldsymbol{C}_3|\big|\boldsymbol{C}_3^{-1} + \boldsymbol{C}_4\boldsymbol{C}_1^{-1}\boldsymbol{C}_2\big|, \tag{15}$$

with $\boldsymbol{C}_i$, $i = 1, 2, 3$, being an arbitrary matrix of appropriate orders. Nulling the derivative of (14) w.r.t. $\boldsymbol{Q}$, after some algebra, yields the MLE of $\boldsymbol{Q}$ under H_0

$$\hat{\boldsymbol{Q}}_0 = (\tilde{\boldsymbol{J}}^H\tilde{\boldsymbol{J}})^{-1}\tilde{\boldsymbol{J}}^H\tilde{\boldsymbol{X}}, \tag{16}$$

where $\tilde{\boldsymbol{X}} = \boldsymbol{S}^{-1/2}\boldsymbol{X}$ and $\tilde{\boldsymbol{J}} = \boldsymbol{S}^{-1/2}\boldsymbol{J}$. In view of (16), we have

$$\tilde{\boldsymbol{X}} - \tilde{\boldsymbol{J}}\hat{\boldsymbol{Q}}_0 = \boldsymbol{P}_{\tilde{\boldsymbol{J}}}^\perp\tilde{\boldsymbol{X}}. \tag{17}$$

Applying the matrix inversion lemma ([38], p. 534) to (13) and utilizing (17) leads to

$$\hat{\boldsymbol{R}}_0^{-1} = (K+L)\boldsymbol{S}^{-1/2}\Big[\boldsymbol{I}_N - \boldsymbol{P}_{\tilde{\boldsymbol{J}}}^\perp\tilde{\boldsymbol{X}}(\sigma^2\boldsymbol{I}_K + \tilde{\boldsymbol{X}}^H\boldsymbol{P}_{\tilde{\boldsymbol{J}}}^\perp\tilde{\boldsymbol{X}})^{-1}\tilde{\boldsymbol{X}}^H\boldsymbol{P}_{\tilde{\boldsymbol{J}}}^\perp\Big]\boldsymbol{S}^{-1/2}. \tag{18}$$

It follows from (18) that

$$(\boldsymbol{H}^H\hat{\boldsymbol{R}}_0^{-1}\boldsymbol{H})^{-1} = \sigma^2\Big[\tilde{\boldsymbol{H}}^H\tilde{\boldsymbol{H}} - \tilde{\boldsymbol{H}}^H\boldsymbol{P}_{\tilde{\boldsymbol{J}}}^\perp\tilde{\boldsymbol{X}}(\sigma^2\boldsymbol{I}_K + \tilde{\boldsymbol{X}}^H\boldsymbol{P}_{\tilde{\boldsymbol{J}}}^\perp\tilde{\boldsymbol{X}})^{-1}\tilde{\boldsymbol{X}}^H\boldsymbol{P}_{\tilde{\boldsymbol{J}}}^\perp\tilde{\boldsymbol{H}}\Big]^{-1}$$
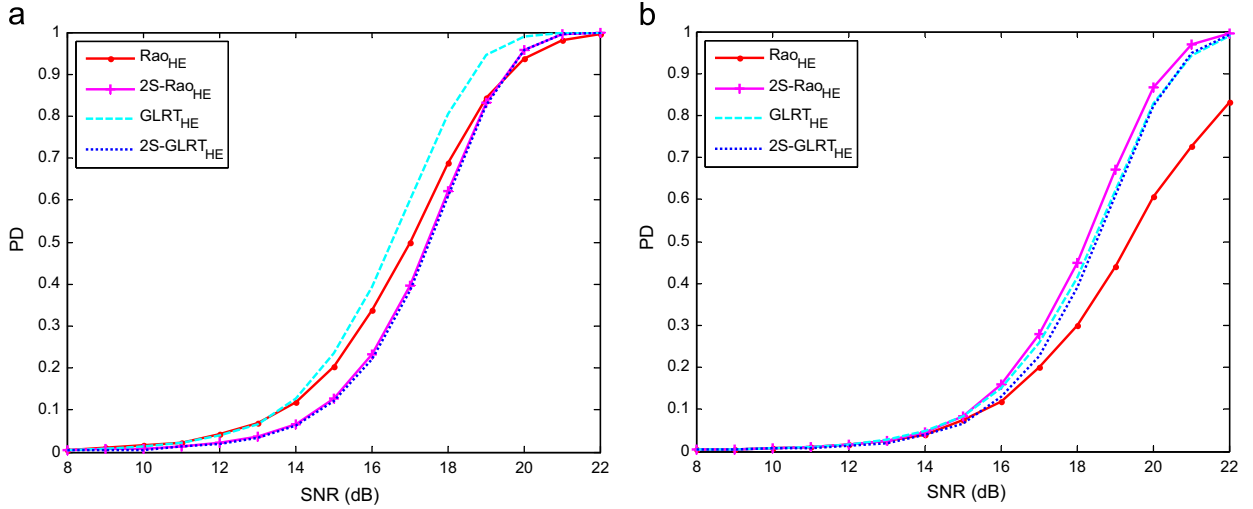
Fig. 1. PD versus SNR in the HE. $p = 7$, $K = 4$, $L = 2N$, and INR = 15 dB. (a) q=1, (b) q=5.

$$= \sigma^2 \Big[(\tilde{\boldsymbol{H}}^H \tilde{\boldsymbol{H}})^{-1} + (\tilde{\boldsymbol{H}}^H \tilde{\boldsymbol{H}})^{-1} \tilde{\boldsymbol{H}}^H \boldsymbol{P}_{\tilde{\boldsymbol{J}}}^\perp \tilde{\boldsymbol{X}} (\sigma^2 \boldsymbol{I}_K$$
$$+ \tilde{\boldsymbol{X}}^H \boldsymbol{P}_{\tilde{\boldsymbol{J}}}^\perp \boldsymbol{P}_{\tilde{\boldsymbol{H}}}^\perp \boldsymbol{P}_{\tilde{\boldsymbol{J}}}^\perp \tilde{\boldsymbol{X}})^{-1} \tilde{\boldsymbol{X}}^H \boldsymbol{P}_{\tilde{\boldsymbol{J}}}^\perp \tilde{\boldsymbol{H}} (\tilde{\boldsymbol{H}}^H \tilde{\boldsymbol{H}})^{-1} \Big], \tag{19}$$

where $\tilde{\boldsymbol{H}} = \boldsymbol{S}^{-1/2} \boldsymbol{H}$. Plugging (17)–(19) into (12), after some algebra, yields the Rao test for known σ^2

$$t_{Rao|\sigma^2} = tr \Big\{ \tilde{\boldsymbol{X}}^H \boldsymbol{P}_{\tilde{\boldsymbol{J}}}^\perp \Big[\boldsymbol{I}_N - \tilde{\boldsymbol{X}} (\sigma^2 \boldsymbol{I}_K + \tilde{\boldsymbol{X}}^H \boldsymbol{P}_{\tilde{\boldsymbol{J}}}^\perp \tilde{\boldsymbol{X}})^{-1} \tilde{\boldsymbol{X}}^H \Big] \boldsymbol{P}_{\tilde{\boldsymbol{J}}}^\perp \boldsymbol{P}_{\tilde{\boldsymbol{H}}}$$
$$\cdot \Big[\boldsymbol{I}_N + \boldsymbol{P}_{\tilde{\boldsymbol{J}}}^\perp \tilde{\boldsymbol{X}} (\sigma^2 \boldsymbol{I}_K + \tilde{\boldsymbol{X}}^H \boldsymbol{P}_{\tilde{\boldsymbol{J}}}^\perp \boldsymbol{P}_{\tilde{\boldsymbol{H}}}^\perp \boldsymbol{P}_{\tilde{\boldsymbol{J}}}^\perp \tilde{\boldsymbol{X}})^{-1} \tilde{\boldsymbol{X}}^H \boldsymbol{P}_{\tilde{\boldsymbol{J}}}^\perp \Big] \boldsymbol{P}_{\tilde{\boldsymbol{H}}} \boldsymbol{P}_{\tilde{\boldsymbol{J}}}^\perp$$
$$\cdot \Big[\boldsymbol{I}_N - \tilde{\boldsymbol{X}} (\sigma^2 \boldsymbol{I}_K + \tilde{\boldsymbol{X}}^H \boldsymbol{P}_{\tilde{\boldsymbol{J}}}^\perp \tilde{\boldsymbol{X}})^{-1} \tilde{\boldsymbol{X}}^H \Big] \boldsymbol{P}_{\tilde{\boldsymbol{J}}}^\perp \tilde{\boldsymbol{X}} \Big\} / \sigma^2. \tag{20}$$

Setting $\sigma^2 = 1$ in (20) results in the Rao test in the HE, which, as shown in the appendix, can be written in the compact form[2]

$$t_{Rao_h} = tr \Big[(\boldsymbol{I}_K + \tilde{\boldsymbol{X}}^H \boldsymbol{P}_{\tilde{\boldsymbol{J}}}^\perp \tilde{\boldsymbol{X}})^{-1} \tilde{\boldsymbol{X}}^H \boldsymbol{P}_{\tilde{\boldsymbol{J}}}^\perp \boldsymbol{P}_{\tilde{\boldsymbol{H}}} \boldsymbol{P}_{\tilde{\boldsymbol{J}}}^\perp \tilde{\boldsymbol{X}} (\boldsymbol{I}_K$$
$$+ \tilde{\boldsymbol{X}}^H \boldsymbol{P}_{\tilde{\boldsymbol{J}}}^\perp \boldsymbol{P}_{\tilde{\boldsymbol{H}}}^\perp \boldsymbol{P}_{\tilde{\boldsymbol{J}}}^\perp \tilde{\boldsymbol{X}})^{-1} \Big]. \tag{21}$$

According to [1] or [6], the MLE of σ^2 under H_0, denoted as $\hat{\sigma}_0^2$, is the unique positive solution to the equation,

$$NK/(K+L) - \sum_{k=1}^{t} \lambda_{k,0}/(\lambda_{k,0} + x) = 0, \tag{22}$$

where x denotes the unknown, $t = \min(N, K)$, and $\lambda_{k,0}$ is the kth non-zero eigenvalue of $\tilde{\boldsymbol{X}}^H \boldsymbol{P}_{\tilde{\boldsymbol{J}}}^\perp \tilde{\boldsymbol{X}}$.

Replacing $\boldsymbol{BD}$ by $\boldsymbol{JQ}$ in (7), then nulling its derivative $\boldsymbol{Q}$. r.t. $\boldsymbol{Q}$ yields the MLE of $\boldsymbol{Q}$ for given $\boldsymbol{R}$ under H_0

$$\hat{\boldsymbol{Q}}_0 = (\bar{\boldsymbol{J}}^H \bar{\boldsymbol{J}})^{-1} \bar{\boldsymbol{J}}^H \overline{\boldsymbol{X}}, \tag{23}$$

where $\bar{\boldsymbol{J}} = \boldsymbol{R}^{-1/2} \boldsymbol{J}$ and $\overline{\boldsymbol{X}} = \boldsymbol{R}^{-1/2} \boldsymbol{X}$. Plugging (23) into (12) leads to the Rao test for given $\boldsymbol{R}$ and σ^2,

$$t_{Rao|\boldsymbol{R},\sigma^2} = tr(\overline{\boldsymbol{X}}^H \boldsymbol{P}_{\bar{\boldsymbol{J}}}^\perp \boldsymbol{P}_{\bar{\boldsymbol{H}}} \boldsymbol{P}_{\bar{\boldsymbol{J}}}^\perp \overline{\boldsymbol{X}})/\sigma^2. \tag{24}$$

Inserting (16) and $\hat{\sigma}_0^2$ into (13) results in

$$\hat{\boldsymbol{R}}_0 = \boldsymbol{S}^{1/2} (\boldsymbol{I}_N + \boldsymbol{P}_{\tilde{\boldsymbol{J}}}^\perp \tilde{\boldsymbol{X}} \tilde{\boldsymbol{X}}^H \boldsymbol{P}_{\tilde{\boldsymbol{J}}}^\perp / \hat{\sigma}_0^2) \boldsymbol{S}^{1/2} / (K+L). \tag{25}$$

Substituting $\hat{\sigma}_0^2$ and (25) into (20) yields the final Rao test in the PHE

$$t_{Rao_{ph}} = tr(\check{\boldsymbol{X}}^H \boldsymbol{P}_{\check{\boldsymbol{J}}}^\perp \boldsymbol{P}_{\check{\boldsymbol{H}}} \boldsymbol{P}_{\check{\boldsymbol{J}}}^\perp \check{\boldsymbol{X}})/\hat{\sigma}_0^2, \tag{26}$$

where $\check{\boldsymbol{X}} = \hat{\boldsymbol{R}}_0^{-1/2} \boldsymbol{X}$, $\check{\boldsymbol{J}} = \hat{\boldsymbol{R}}_0^{-1/2} \boldsymbol{J}$, and $\check{\boldsymbol{H}} = \hat{\boldsymbol{R}}_0^{-1/2} \boldsymbol{H}$.

3.2. Two-step Rao test

For the two-step detector design, it is first assumed that the covariance matrix (in the HE) or only its structure (in the PHE) is known, and a detector according to a certain criterion is devised. Then the covariance matrix or its structure is replaced by a proper estimate [1]. Setting $\sigma^2 = 1$ in (24) and substituting $\boldsymbol{S}$ for the implicitly used $\boldsymbol{R}$ yields the 2S-Rao test in the HE

$$t_{2S-Rao_h} = tr(\tilde{\boldsymbol{X}}^H \boldsymbol{P}_{\tilde{\boldsymbol{J}}}^\perp \boldsymbol{P}_{\tilde{\boldsymbol{H}}} \boldsymbol{P}_{\tilde{\boldsymbol{J}}}^\perp \tilde{\boldsymbol{X}}). \tag{27}$$

To obtain the 2S-Rao test in the PHE, we need to derive the MLE of σ^2 for given $\boldsymbol{R}$ under H_0. Inserting (23) into (7), setting $\boldsymbol{P} = \boldsymbol{0}_{p \times K}$, and ignoring the PDF of $\boldsymbol{X}_L$ results in

$$f_0(\boldsymbol{X}; \hat{\boldsymbol{Q}}_0) = (\pi^N \sigma^{2N} |\boldsymbol{R}|)^{-K} \exp \Big[-tr(\overline{\boldsymbol{X}}^H \boldsymbol{P}_{\bar{\boldsymbol{J}}}^\perp \overline{\boldsymbol{X}})/\sigma^2 \Big]. \tag{28}$$

Nulling the derivative of (28) w.r.t. σ^2 leads to the MLE of σ^2 for given $\boldsymbol{R}$ under H_0

$$\hat{\sigma}_0^2 = tr(\overline{\boldsymbol{X}}^H \boldsymbol{P}_{\bar{\boldsymbol{J}}}^\perp \overline{\boldsymbol{X}})/NK. \tag{29}$$

Substituting (29) into (24) and dropping the constant yields the Rao test for given $\boldsymbol{R}$ in the PHE

$$t_{Rao_{ph}|\boldsymbol{R}} = tr(\overline{\boldsymbol{X}}^H \boldsymbol{P}_{\bar{\boldsymbol{J}}}^\perp \boldsymbol{P}_{\bar{\boldsymbol{H}}} \boldsymbol{P}_{\bar{\boldsymbol{J}}}^\perp \overline{\boldsymbol{X}})/tr(\overline{\boldsymbol{X}}^H \boldsymbol{P}_{\bar{\boldsymbol{J}}}^\perp \overline{\boldsymbol{X}}). \tag{30}$$

Replacing the implicitly used $\boldsymbol{R}$ in (30) by $\boldsymbol{S}$ results in the final 2S-Rao test in the PHE

$$t_{2S-Rao_{ph}} = tr(\tilde{\boldsymbol{X}}^H \boldsymbol{P}_{\tilde{\boldsymbol{J}}}^\perp \boldsymbol{P}_{\tilde{\boldsymbol{H}}} \boldsymbol{P}_{\tilde{\boldsymbol{J}}}^\perp \tilde{\boldsymbol{X}})/tr(\tilde{\boldsymbol{X}}^H \boldsymbol{P}_{\tilde{\boldsymbol{J}}}^\perp \tilde{\boldsymbol{X}}). \tag{31}$$

Remarkably, all the proposed detectors are CFAR. Precisely, the detectors (21) and (27) in the HE are CFAR w.r.t. the noise covariance matrix $\boldsymbol{R}$, and the detectors (26) and (31) in the PHE are CFAR w.r.t. $\boldsymbol{R}$ and σ^2. This can be proved

---

[2] To distinguish the detectors for the HE and PHE, we add "h" and "ph" in the corresponding subscripts of them.
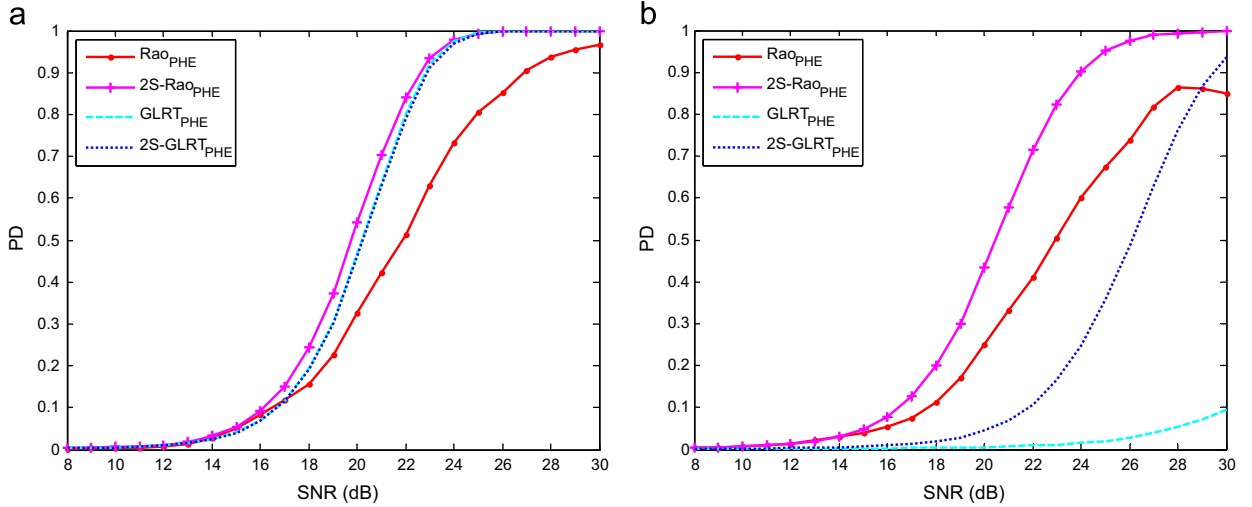
Fig. 2. PD versus SNR in the PHE. $p=8$, $K=4$, $L=2N$, and INR $=15$ dB. (a) q=1, (b) q=3.

in a manner analogous to [1,39]. For simplicity, the details are omitted here.

4. Simulation results

In this section, we assess the detection performance of the proposed detectors by Monte Carlo simulation. To obtain the detection threshold for a preassigned probability of false alarm (PFA), 100/PFA data realizations are performed. To determine the probability of detection (PD), 10^4 data realizations are used. The signal-to-noise ratio (SNR) and interference-to-noise ratio (INR) are defined as

$$SNR = tr(\boldsymbol{P}^H \boldsymbol{H}^H \boldsymbol{R}^{-1} \boldsymbol{H} \boldsymbol{P}) \tag{32}$$

and

$$INR = tr(\boldsymbol{Q}^H \boldsymbol{J}^H \boldsymbol{R}^{-1} \boldsymbol{J} \boldsymbol{Q}), \tag{33}$$

respectively. Throughout this section we set $N=12$ and PFA $=10^{-3}$, and the INR is set to be 15 dB in all figures except Fig. 7. Moreover, the (i,j)th element of $\boldsymbol{R}$ is chosen as $0.96^{abs(i-j)}$. In the PHE, we choose $\sigma^2 = 2$. The matrices $\boldsymbol{H}$ and $\boldsymbol{J}$ are randomly chosen. After being generated, they are fixed in each Monte Carlo simulation.

For comparison purposes, the PDs of the GLRT and 2S-GLRT for the detection problem in (1) are also provided. The GLRT and 2S-GLRT in the HE are [25]

$$t_{GLRT_h} = \left| \boldsymbol{I}_K + \tilde{\boldsymbol{X}}^H \boldsymbol{P}_{\tilde{\boldsymbol{J}}}^{\perp} \tilde{\boldsymbol{X}} \right| / \left| \boldsymbol{I}_K + \tilde{\boldsymbol{X}}^H \boldsymbol{P}_{\tilde{\boldsymbol{B}}}^{\perp} \tilde{\boldsymbol{X}} \right| \tag{34}$$

and

$$t_{2S-GLRT_h} = tr\left[\tilde{\boldsymbol{X}}^H (\boldsymbol{P}_{\tilde{\boldsymbol{B}}} - \boldsymbol{P}_{\tilde{\boldsymbol{J}}}) \tilde{\boldsymbol{X}} \right], \tag{35}$$

respectively. Moreover, the GLRT and 2S-GLRT in the PHE are [25]

$$t_{GLRT_{ph}} = \frac{\left(\hat{\sigma}_0^2 \right)^{NK/(K+L)} \left| \boldsymbol{I}_K + \tilde{\boldsymbol{X}}^H \boldsymbol{P}_{\tilde{\boldsymbol{J}}}^{\perp} \tilde{\boldsymbol{X}} / \hat{\sigma}_0^2 \right|}{\left(\hat{\sigma}_1^2 \right)^{NK/(K+L)} \left| \boldsymbol{I}_K + \tilde{\boldsymbol{X}}^H \boldsymbol{P}_{\tilde{\boldsymbol{B}}}^{\perp} \tilde{\boldsymbol{X}} / \hat{\sigma}_1^2 \right|} \tag{36}$$

and

$$t_{2S-GLRT_{ph}} = tr(\tilde{\boldsymbol{X}}^H \boldsymbol{P}_{\tilde{\boldsymbol{J}}}^{\perp} \tilde{\boldsymbol{X}}) / tr(\tilde{\boldsymbol{X}}^H \boldsymbol{P}_{\tilde{\boldsymbol{B}}}^{\perp} \tilde{\boldsymbol{X}}), \tag{37}$$

respectively. In (36), $\hat{\sigma}_0^2$ is the sole solution to (22), and $\hat{\sigma}_1^2$ is the sole solution to the equation

$$NK/(K+L) - \sum_{k=1}^{t} \lambda_{k,1}/(\lambda_{k,1}+x) = 0, \tag{38}$$

where x is the unknown, $t = \min(N,K)$, $\lambda_{k,1}$ is the kth non-zero eigenvalue of $\tilde{\boldsymbol{X}}^H \boldsymbol{P}_{\tilde{\boldsymbol{B}}}^{\perp} \tilde{\boldsymbol{X}}$, with $\tilde{\boldsymbol{B}} = \boldsymbol{S}^{-1/2} \boldsymbol{B}$ and $\boldsymbol{B} = [\boldsymbol{H}, \boldsymbol{J}]$.

Fig. 1 shows the detection performance of the detectors in the HE. The subscript "HE" indicates that a detector is proposed for the HE. Similarly, "PHE" denotes a detector is devised for the PHE. It is seen that the 2S-Rao test offers the highest PD for $q=5$. Moreover, the PD of each detector decreases with the increase of q. Essentially, this is due to the increase of the loss of the signal energy projected onto the interference subspace.

Fig. 2 displays the detection performance of the detectors in the PHE. The results show that for the chosen parameters the 2S-Rao test achieves a higher PD than the other detectors. Noticeably, the PD of the Rao test in the PHE for $q=3$ is not a monotonically increasing function of the SNR. This phenomenon is more clearly shown in Fig. 3. This result is consistent with that in [40,41]. An intuitive interpretation is that the Rao test is originally proposed for the case of low SNR and a large number of secondary data ([38], p. 208–217, p. 232–234).

The aforementioned phenomenon disappears when the number of the secondary data is large enough, as shown in Fig. 4. Precisely, Fig. 4 indicates that for the case of sufficient secondary data the PDs of the Rao test in the HE and PHE monotonically increase as the SNR becomes larger.
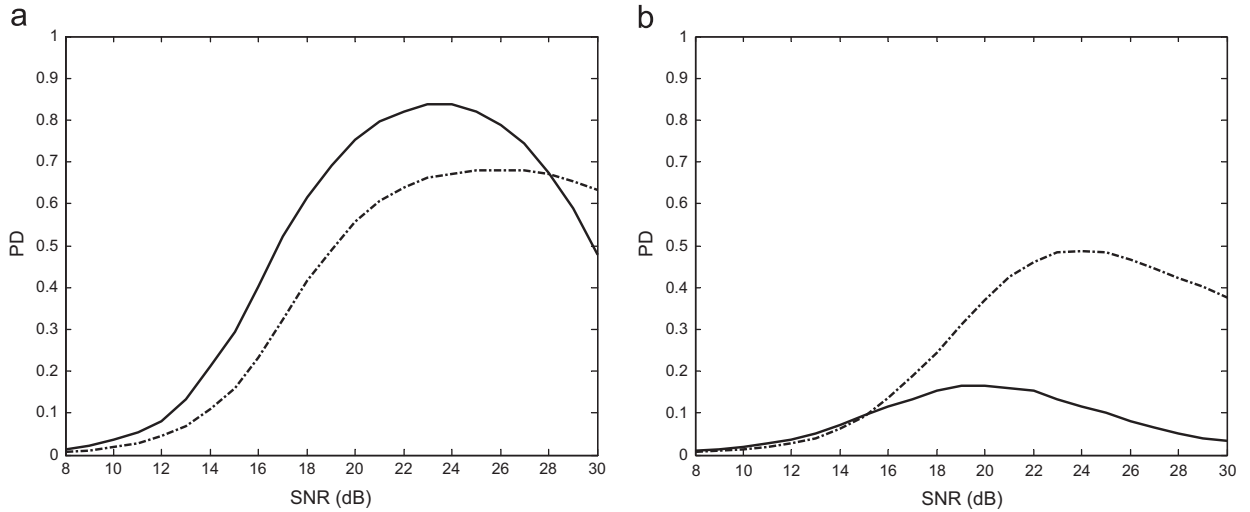
Fig. 3. PDs of the Rao test in the HE and PHE under different SNRs. $L = 2N$ and INR = 15 dB. In (a) the parameters for the Rao test, indicated by the solid line, are $p = 5$, $q = 3$, and $K = 2$, while the parameters for the Rao test, indicated by the dashed-dot line, are $p = 9$, $q = 3$, and $K = 2$. In (b) the parameters for the Rao test, indicated by the solid line, are $p = 1$, $q = 1$, and $K = 6$, while the parameters for the Rao test, indicated by the dashed-dot line, are $p = 2$, $q = 2$, and $K = 6$. (a) Rao test in the HE, (b) Rao test in the PHE.
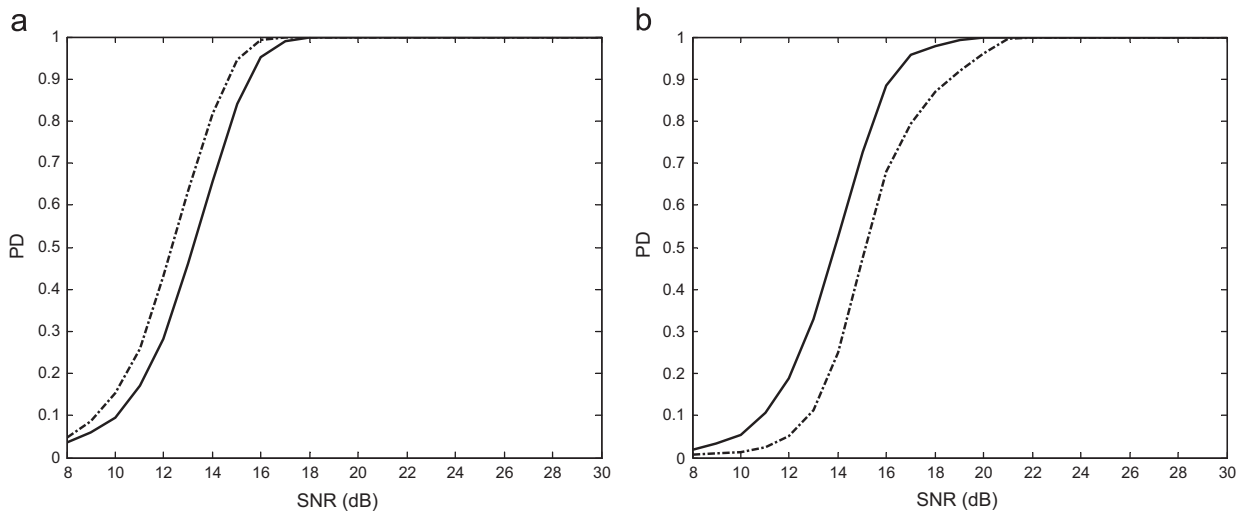
Fig. 4. PDs of the Rao test in the HE and PHE under different SNRs. $L = 14N$ and INR = 15 dB. The values of p, q, and K for the Rao test, indicated by the solid or dash-dot line, are the same as the Rao test in Fig. 3 indicated by corresponding lines. (a) Rao test in the HE, (b) Rao test in PHE.

Fig. 5 compares the performance of the Rao test and GLRT in the HE with known matrix $\boldsymbol{R}$[3]. The values of p, q, and K are the same as Fig. 1. It is indicated in Fig. 5 that the Rao test in the HE for known $\boldsymbol{R}$ is superior to the GLRT when $q = 1$ or $q = 5$.

Fig. 6 is analogous to Fig. 5, but it is for the PHE. It is shown that the Rao test in the PHE for known $\boldsymbol{R}$ has higher PD than the GLRT. Particularly, at PD = 0.9 the performance improvement of the Rao test over the GLRT in terms of SNR is nearly 5 dB.

---

[3] Setting $\sigma^2 = 1$ in (24) we obtain the Rao test in the HE for known $\boldsymbol{R}$. Replacing $\tilde{\boldsymbol{X}}$, $\tilde{\boldsymbol{B}}$, and $\tilde{\boldsymbol{J}}$ in (35) by $\overline{\boldsymbol{X}}$, $\overline{\boldsymbol{B}}$, $\overline{\boldsymbol{J}}$, respectively, results in the GLRT in the HE for known $\boldsymbol{R}$. Moreover, the Rao test for the case of known $\boldsymbol{R}$ in the PHE is given in (30). The GLRT for known $\boldsymbol{R}$ in the PHE is obtained when $\tilde{\boldsymbol{X}}$, $\tilde{\boldsymbol{B}}$, and $\tilde{\boldsymbol{J}}$ in (37) are replaced by $\overline{\boldsymbol{X}}$, $\overline{\boldsymbol{B}}$, and $\overline{\boldsymbol{J}}$, respectively.

Fig. 7 depicts the PDs of the detectors for different INRs. It is seen that the PDs are nearly unaltered with the increase of the INR. In other words, all the detectors can successfully reject the interference. Together with the results in Figs. 1–6, we see that the detection performance of the detectors are mainly affected by the dimension of the interference subspace, instead of the power of the interference.

Note that the number of the range bins that the distributed target occupies, i.e., K, is assumed to be exactly known in the simulations above. However, there may be a mismatch between the actual value of K and the nominal one. When the mismatch arises, the actual value of K, denoted as K_a, is not equal to the nominal K, denoted as K_n. In particular, the phenomenon of signal contamination would happen if $K_a > K_n$, i.e., the data collected from some range bins the target occupies are taken as a portion of the
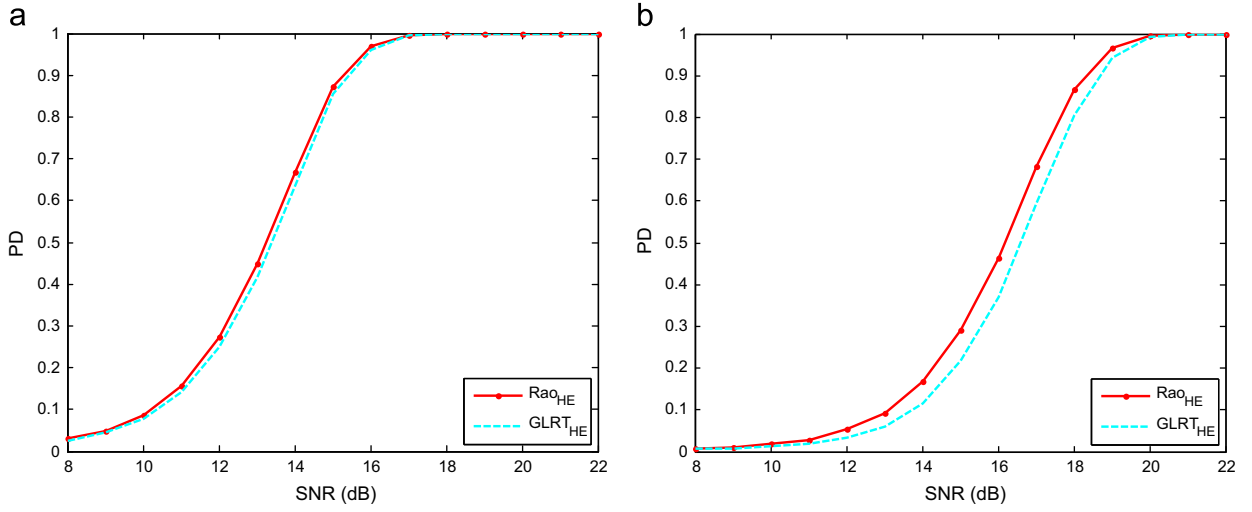
Fig. 5. PD versus SNR in the HE for known **R**. $p = 7$, $K = 4$, and INR = 15 dB. (a) q=1, (b) q=5.
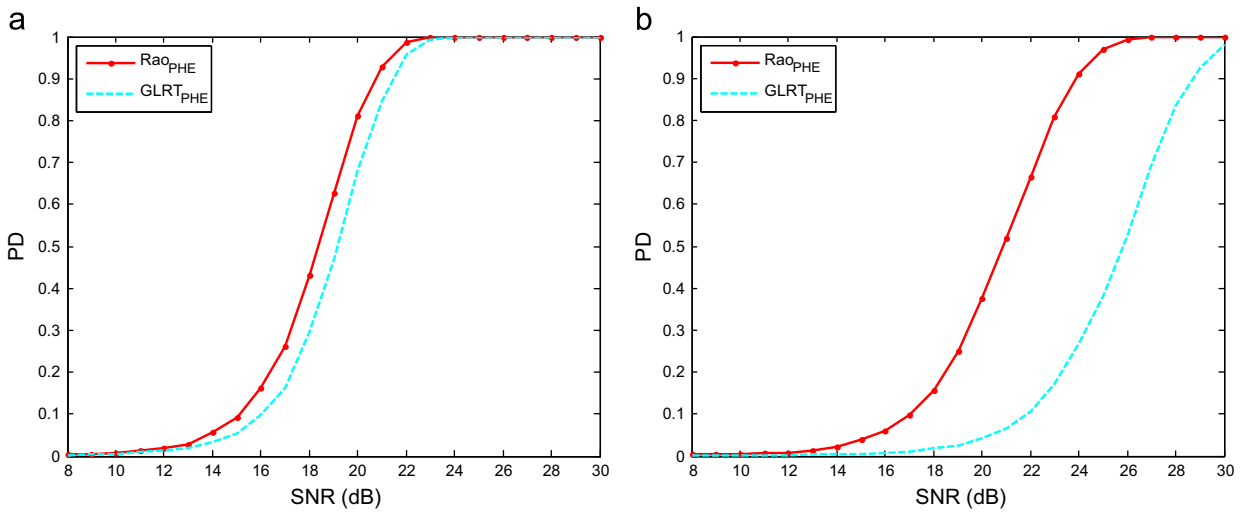
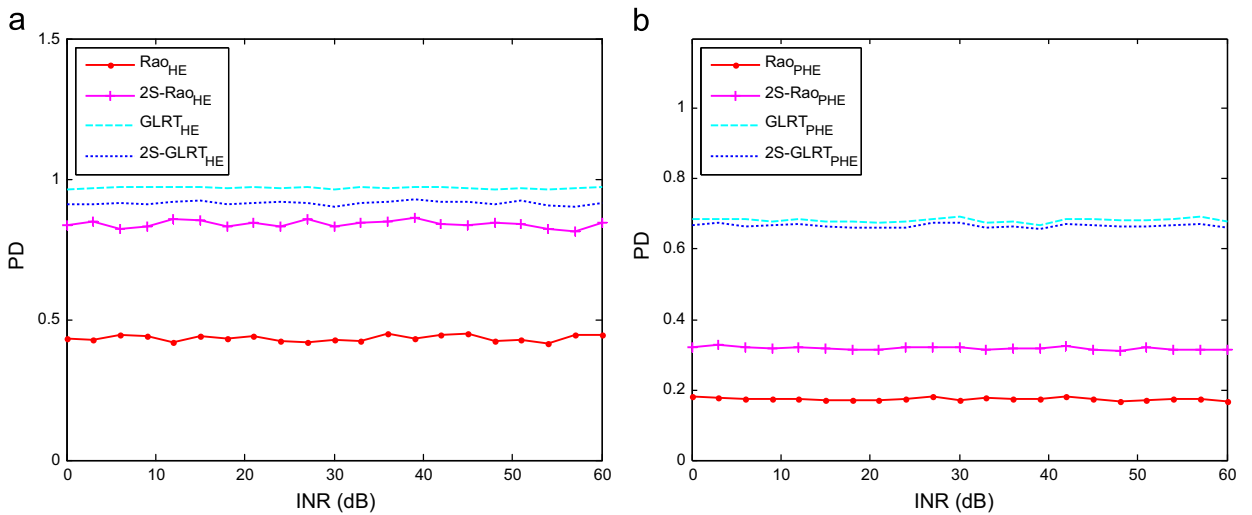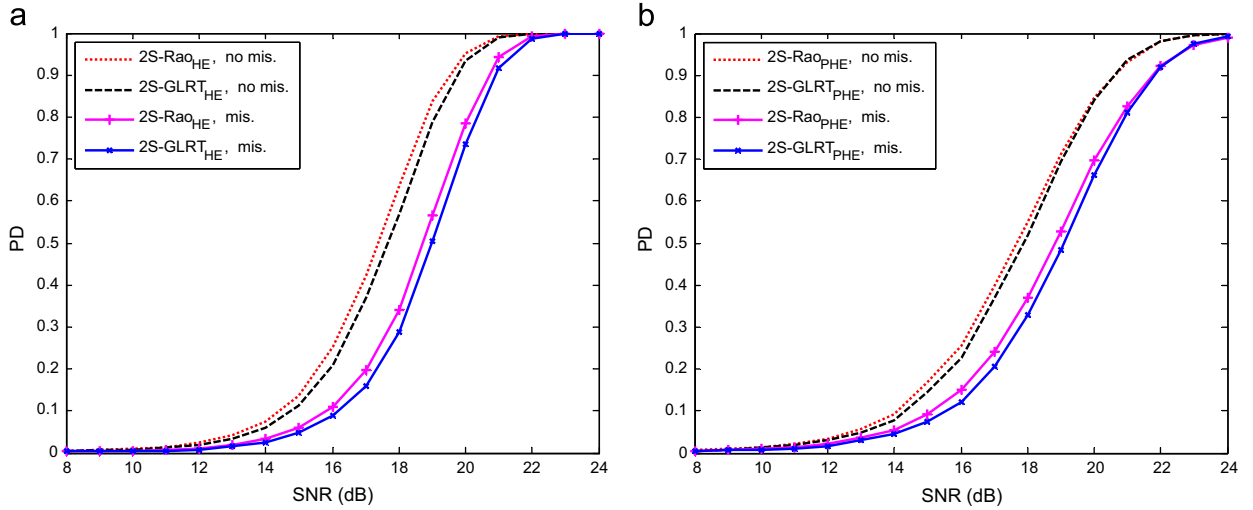**Fig. 6.** PD versus SNR in the PHE for known **R**. $p = 8$, $K = 4$, and INR = 15 dB. (a) q=1, (b) q=3.

Fig. 7. PD versus INR. $p = 4$, $q = 3$, $K = 6$, $L = 2N$, and SNR = 20 dB. (a) HE, (b) PHE.

Fig. 8. PD versus SNR in the case of mismatch between K_a and K_n. (a) $p=8$, $q=3$, $K_a=6$, $K_n=4$, $L=2N$, INR=15 dB, and cSNR=16 dB. (b) $p=6$, $q=1$, $K_a=4$, $K_n=3$, $L=2N$, INR=15 dB, and cSNR=16 dB. (a) HE, (b) PHE.

training data. To quantify the mismatch, we define the contaminated SNR (cSNR) as $cSNR = \sum_{k=1}^{\Delta K} s_{c,k}^H R^{-1} s_{c,k}/L$, where $\Delta K = K_a - K_n$ and $s_{c,k}$, lying in the subspace spanned by the columns of H, is the signal component in the kth signal-contaminated range bin.

Fig. 8 investigates the detection performance of the detectors when signal contamination occurs, where "no mis." and "mis." denote the matched and mismatched cases, respectively. Only the 2S-Rao and 2S-GLRT are shown to avoid squeezing too many curves in Fig. 8. It is seen that the signal contamination degrades detection performance of the detectors, and the 2S-Rao can provide a slightly higher PD than the 2S-GLRT in the HE and PHE. Essentially, the performance degradation is owing to the raise of the detection thresholds, caused by the signal-contaminated training data.

5. Conclusions

In this paper, we have considered the distributed target detection in interference and noise. We have derived the one-step Rao test and two-step Rao test both in the HE and PHE, all of which have the CFAR property. It is shown that the detectors can effectively reject the interference and detect a target. However, the detection performance degrades with the increase of the interference subspace dimension. The proposed 2S-Rao test in the HE can provide higher PD than the existing GLRT and 2S-GLRT in some situations. Similarly, the proposed 2S-Rao test in the PHE can achieve the best detection performance.

Appendix. Derivation of (21)

In the HE (i.e.,$\sigma^2=1$), (20) becomes

$$t_{Rao_h} = tr\left[\tilde{X}^H P_{\bar{j}}^{\perp}(I_N - E)P_{\bar{j}}^{\perp} P_{\bar{H}}(I_N + F)P_{\bar{H}}P_{\bar{j}}^{\perp}(I_N - E)P_{\bar{j}}^{\perp}\tilde{X}\right], \tag{39}$$

where

$$E = \tilde{X}(I_K + \tilde{X}^H P_{\bar{j}}^{\perp}\tilde{X})^{-1}\tilde{X}^H, \tag{40}$$

$$F = P_{\bar{j}}^{\perp}\tilde{X}(I_K + \tilde{X}^H P_{\bar{j}}^{\perp} P_{\bar{H}}P_{\bar{j}}^{\perp}\tilde{X})^{-1}\tilde{X}^H P_{\bar{j}}^{\perp}. \tag{41}$$

It is straightforward to extend (39) as

$$t_{Rao_h} = tr(G_1 + G_2 - G_3 - G_4), \tag{42}$$

where

$$G_1 = \tilde{X}^H P_{\bar{j}}^{\perp} P_{\bar{H}}P_{\bar{j}}^{\perp}\tilde{X} - \tilde{X}^H P_{\bar{j}}^{\perp} P_{\bar{H}}P_{\bar{j}}^{\perp} EP_{\bar{j}}^{\perp}\tilde{X}, \tag{43}$$

$$G_2 = \tilde{X}^H P_{\bar{j}}^{\perp} P_{\bar{H}}FP_{\bar{H}}P_{\bar{j}}^{\perp}\tilde{X} - \tilde{X}^H P_{\bar{j}}^{\perp} P_{\bar{H}}FP_{\bar{H}}P_{\bar{j}}^{\perp} EP_{\bar{j}}^{\perp}\tilde{X}, \tag{44}$$

$$G_3 = \tilde{X}^H P_{\bar{j}}^{\perp} EP_{\bar{j}}^{\perp} P_{\bar{H}}P_{\bar{j}}^{\perp}\tilde{X} - \tilde{X}^H P_{\bar{j}}^{\perp} EP_{\bar{j}}^{\perp} P_{\bar{H}}P_{\bar{j}}^{\perp} EP_{\bar{j}}^{\perp}\tilde{X}, \tag{45}$$

$$G_4 = \tilde{X}^H P_{\bar{j}}^{\perp} EP_{\bar{j}}^{\perp} P_{\bar{H}}FP_{\bar{H}}P_{\bar{j}}^{\perp}\tilde{X}\tilde{X}^H P_{\bar{j}}^{\perp} EP_{\bar{j}}^{\perp} P_{\bar{H}}FP_{\bar{H}}P_{\bar{j}}^{\perp} EP_{\bar{j}}^{\perp}\tilde{X}. \tag{46}$$

We observe that

$$\tilde{X} - EP_{\bar{j}}^{\perp}\tilde{X} = \tilde{X}\left[I_K - (I_K + \tilde{X}^H P_{\bar{j}}^{\perp}\tilde{X})^{-1}\tilde{X}^H P_{\bar{j}}^{\perp}\tilde{X}\right]. \tag{47}$$

Moreover, according to the following identity (see e.g., [42])

$$I_N - (I_N + L)^{-1}L = (I_N + L)^{-1}, \tag{48}$$

with L being an $N \times N$ matrix, (47) can be recast as

$$\tilde{X} - EP_{\bar{j}}^{\perp}\tilde{X} = \tilde{X}(I_K + \tilde{X}^H P_{\bar{j}}^{\perp}\tilde{X})^{-1}. \tag{49}$$

It follows that (43)–(46) can be represented by

$$G_1 = \tilde{X}^H P_{\bar{j}}^{\perp} P_{\bar{H}}P_{\bar{j}}^{\perp}\tilde{X}(I_K + \tilde{X}^H P_{\bar{j}}^{\perp}\tilde{X})^{-1}, \tag{50}$$

$$G_2 = \tilde{X}^H P_{\bar{j}}^{\perp} P_{\bar{H}}FP_{\bar{H}}P_{\bar{j}}^{\perp}\tilde{X}(I_K + \tilde{X}^H P_{\bar{j}}^{\perp}\tilde{X})^{-1}, \tag{51}$$

$$G_3 = \tilde{X}^H P_{\bar{j}}^{\perp} EP_{\bar{j}}^{\perp} P_{\bar{H}}P_{\bar{j}}^{\perp}\tilde{X}(I_K + \tilde{X}^H P_{\bar{j}}^{\perp}\tilde{X})^{-1}, \tag{52}$$

and

$$\boldsymbol{G}_4 = \tilde{\boldsymbol{X}}^H \boldsymbol{P}_{\tilde{j}}^{\perp} \boldsymbol{E} \boldsymbol{P}_{\tilde{j}}^{\perp} \boldsymbol{P}_{\tilde{H}} \boldsymbol{F} \boldsymbol{P}_{\tilde{H}} \boldsymbol{P}_{\tilde{j}}^{\perp} \tilde{\boldsymbol{X}} (\boldsymbol{I}_K + \tilde{\boldsymbol{X}}^H \boldsymbol{P}_{\tilde{j}}^{\perp} \tilde{\boldsymbol{X}})^{-1}. \tag{53}$$

respectively. In a similar manner, we have

$$\boldsymbol{G}_1 - \boldsymbol{G}_3 = (\boldsymbol{I}_K + \tilde{\boldsymbol{X}}^H \boldsymbol{P}_{\tilde{j}}^{\perp} \tilde{\boldsymbol{X}})^{-1} \tilde{\boldsymbol{X}}^H \boldsymbol{P}_{\tilde{j}}^{\perp} \boldsymbol{P}_{\tilde{H}} \boldsymbol{P}_{\tilde{j}}^{\perp} \tilde{\boldsymbol{X}} (\boldsymbol{I}_K + \tilde{\boldsymbol{X}}^H \boldsymbol{P}_{\tilde{j}}^{\perp} \tilde{\boldsymbol{X}})^{-1}, \tag{54}$$

$$\boldsymbol{G}_2 - \boldsymbol{G}_4 = (\boldsymbol{I}_K + \tilde{\boldsymbol{X}}^H \boldsymbol{P}_{\tilde{j}}^{\perp} \tilde{\boldsymbol{X}})^{-1} \tilde{\boldsymbol{X}}^H \boldsymbol{P}_{\tilde{j}}^{\perp} \boldsymbol{P}_{\tilde{H}} \boldsymbol{F} \boldsymbol{P}_{\tilde{H}} \boldsymbol{P}_{\tilde{j}}^{\perp} \tilde{\boldsymbol{X}} (\boldsymbol{I}_K + \tilde{\boldsymbol{X}}^H \boldsymbol{P}_{\tilde{j}}^{\perp} \tilde{\boldsymbol{X}})^{-1}. \tag{55}$$

Furthermore, it follows from (41) that

$$\begin{aligned}
\tilde{\boldsymbol{X}}^H \boldsymbol{P}_{\tilde{j}}^{\perp} \boldsymbol{P}_{\tilde{H}} \boldsymbol{P}_{\tilde{j}}^{\perp} \tilde{\boldsymbol{X}} &+ \tilde{\boldsymbol{X}}^H \boldsymbol{P}_{\tilde{j}}^{\perp} \boldsymbol{P}_{\tilde{H}} \boldsymbol{F} \boldsymbol{P}_{\tilde{H}} \boldsymbol{P}_{\tilde{j}}^{\perp} \tilde{\boldsymbol{X}} = \tilde{\boldsymbol{X}}^H \boldsymbol{P}_{\tilde{j}}^{\perp} \boldsymbol{P}_{\tilde{H}} \boldsymbol{P}_{\tilde{j}}^{\perp} \tilde{\boldsymbol{X}} \big[\boldsymbol{I}_K \\
&+ (\boldsymbol{I}_K + \tilde{\boldsymbol{X}}^H \boldsymbol{P}_{\tilde{H}}^{\perp} \boldsymbol{P}_{\tilde{j}}^{\perp} \tilde{\boldsymbol{X}})^{-1} \tilde{\boldsymbol{X}}^H \boldsymbol{P}_{\tilde{j}}^{\perp} (\boldsymbol{I}_N - \boldsymbol{P}_{\tilde{H}}^{\perp}) \boldsymbol{P}_{\tilde{j}}^{\perp} \tilde{\boldsymbol{X}} \big] \\
&= \tilde{\boldsymbol{X}}^H \boldsymbol{P}_{\tilde{j}}^{\perp} \boldsymbol{P}_{\tilde{H}} \boldsymbol{P}_{\tilde{j}}^{\perp} \tilde{\boldsymbol{X}} \big[\boldsymbol{I}_K - (\boldsymbol{I}_K + \tilde{\boldsymbol{X}}^H \boldsymbol{P}_{\tilde{j}}^{\perp} \boldsymbol{P}_{\tilde{H}}^{\perp} \boldsymbol{P}_{\tilde{j}}^{\perp} \tilde{\boldsymbol{X}})^{-1} \tilde{\boldsymbol{X}}^H \boldsymbol{P}_{\tilde{j}}^{\perp} \boldsymbol{P}_{\tilde{H}}^{\perp} \boldsymbol{P}_{\tilde{j}}^{\perp} \tilde{\boldsymbol{X}} \\
&+ (\boldsymbol{I}_K + \tilde{\boldsymbol{X}}^H \boldsymbol{P}_{\tilde{j}}^{\perp} \boldsymbol{P}_{\tilde{H}}^{\perp} \boldsymbol{P}_{\tilde{j}}^{\perp} \tilde{\boldsymbol{X}})^{-1} \tilde{\boldsymbol{X}}^H \boldsymbol{P}_{\tilde{j}}^{\perp} \tilde{\boldsymbol{X}} \big] \\
&= \tilde{\boldsymbol{X}}^H \boldsymbol{P}_{\tilde{j}}^{\perp} \boldsymbol{P}_{\tilde{H}} \boldsymbol{P}_{\tilde{j}}^{\perp} \tilde{\boldsymbol{X}} \big[(\boldsymbol{I}_K + \tilde{\boldsymbol{X}}^H \boldsymbol{P}_{\tilde{j}}^{\perp} \boldsymbol{P}_{\tilde{H}}^{\perp} \boldsymbol{P}_{\tilde{j}}^{\perp} \tilde{\boldsymbol{X}})^{-1} \\
&+ (\boldsymbol{I}_K + \tilde{\boldsymbol{X}}^H \boldsymbol{P}_{\tilde{j}}^{\perp} \boldsymbol{P}_{\tilde{H}}^{\perp} \boldsymbol{P}_{\tilde{j}}^{\perp} \tilde{\boldsymbol{X}})^{-1} \tilde{\boldsymbol{X}}^H \boldsymbol{P}_{\tilde{j}}^{\perp} \tilde{\boldsymbol{X}} \big] \\
&= \tilde{\boldsymbol{X}}^H \boldsymbol{P}_{\tilde{j}}^{\perp} \boldsymbol{P}_{\tilde{H}} \boldsymbol{P}_{\tilde{j}}^{\perp} \tilde{\boldsymbol{X}} (\boldsymbol{I}_K + \tilde{\boldsymbol{X}}^H \boldsymbol{P}_{\tilde{j}}^{\perp} \boldsymbol{P}_{\tilde{H}}^{\perp} \boldsymbol{P}_{\tilde{j}}^{\perp} \tilde{\boldsymbol{X}})^{-1} (\boldsymbol{I}_K + \tilde{\boldsymbol{X}}^H \boldsymbol{P}_{\tilde{j}}^{\perp} \tilde{\boldsymbol{X}}),
\end{aligned} \tag{56}$$

where we have used (48) in the last equality. According to (54)–(56), we have

$$\begin{aligned}
\boldsymbol{G}_1 + \boldsymbol{G}_2 - \boldsymbol{G}_3 - \boldsymbol{G}_4 &= (\boldsymbol{I}_K + \tilde{\boldsymbol{X}}^H \boldsymbol{P}_{\tilde{j}}^{\perp} \tilde{\boldsymbol{X}})^{-1} \tilde{\boldsymbol{X}}^H \boldsymbol{P}_{\tilde{j}}^{\perp} \boldsymbol{P}_{\tilde{H}} \boldsymbol{P}_{\tilde{j}}^{\perp} \tilde{\boldsymbol{X}} (\boldsymbol{I}_K \\
&+ \tilde{\boldsymbol{X}}^H \boldsymbol{P}_{\tilde{j}}^{\perp} \boldsymbol{P}_{\tilde{H}}^{\perp} \boldsymbol{P}_{\tilde{j}}^{\perp} \tilde{\boldsymbol{X}})^{-1}. \tag{57}
\end{aligned}$$

Plugging (57) into (42) results in (21). This finishes the derivation.

References

[1] E. Conte, A.D. Maio, G. Ricci, GLRT-based adaptive detection algorithms for range-spread targets, IEEE Trans. Signal Process. 49 (7) (2001) 1336–1348.

[2] X. Shuai, L. Kong, J. Yang, Adaptive detection for distributed targets in Gaussian noise with Rao and Wald tests, Sci. China Inf. Sci. 55 (6) (2012) 1290–1300.

[3] C. Hao, X. Ma, X. Shang, L. Cai, Adaptive detection of distributed targets in partially homogeneous environment with Rao and Wald tests, Signal Process. 92 (4) (2012) 926–930.

[4] E.J. Kelly, K.M. Forsythe, Adaptive Detection and Parameter Estimation for Multidimensional Signal Models, Lincoln Laboratory, Lexington, 1989.

[5] W. Liu, W. Xie, J. Liu, Y. Wang, Adaptive double subspace signal detection in Gaussian background—Part I: Homogeneous environments, IEEE Trans. Signal Process. 62 (9) (2014) 2345–2357.

[6] W. Liu, W. Xie, J. Liu, Y. Wang, Adaptive double subspace signal detection in Gaussian background—Part II: Partially homogeneous environments, IEEE Trans. Signal Process. 62 (9) (2014) 2358–2369.

[7] J. Carretero-Moya, A.D. Maio, J. Gismero-Menoyo, A. Asensio-López, Experimental performance analysis of distributed target coherent radar detectors, IEEE Trans. Aerosp. Electron. Syst. 48 (3) (2012) 2216–2238.

[8] G. Cui, L. Kong, X. Yang, J. Yang, The Rao and Wald tests designed for distributed targets with polarization MIMO radar in compound-Gaussian clutter, Circuits Syst. Signal Process. 31 (1) (2012) 237–254.

[9] A. Aubry, A.D. Maio, L. Pallotta, A. Farina, Radar detection of distributed targets in homogeneous interference whose inverse covariance structure is defined via unitary invariant functions, IEEE Trans. Signal Process. 61 (20) (2013) 4949–4961.

[10] T. Jian, Y. He, F. Su, X. Huang, D. Ping, Adaptive detection of range-spread targets without secondary data in multichannel autoregressive process, Digital Signal Process. 23 (5) (2013) 1686–1694.

[11] C. Hao, D. Orlando, G. Foglia, X. Ma, S. Yan, C. Hou, Persymmetric adaptive detection of distributed targets in partially-homogeneous environment, Digital Signal Process. 24 (2014) 42–51.

[12] W. Liu, W. Xie, J. Liu, D. Zou, H. Wang, Y. Wang, Detection of a distributed target with direction uncertainty, IET Radar Sonar Navig. 8 (9) (2014) 1177–1183.

[13] Y. Xiao, G. Cui, W. Yi, L. Kong, J. Yang, Adaptive detection and estimation for an unknown occurring interval signal in correlated Gaussian noise, Signal Process. 108 (2015) 440–450.

[14] S.-W. Xu, P.-L. Shui, Y.-H. Cao, Adaptive range-spread maneuvering target detection in compound-Gaussian clutter, Digital Signal Process. 36 (2015) 46–56.

[15] L.L. Scharf, B. Friedlander, Matched subspace detectors, IEEE Trans. Signal Process. 42 (8) (1994) 2146–2156.

[16] R.T. Behrens, L.L. Scharf, Signal processing applications of oblique projection operators, IEEE Trans. Signal Process. 42 (6) (1994) 1413–1424.

[17] L.L. Scharf, M.L. McCloud, Blind adaptation of zero forcing projections and oblique pseudo-inverses for subspace detection and estimation when interference dominates noise, IEEE Trans. Signal Process. 50 (12) (2002) 2938–2946.

[18] J. Liu, Z.-J. Zhang, Y. Cao, M. Wang, Distributed target detection in subspace interference plus Gaussian noise, Signal Process. 85 (2014) 88–100.

[19] O. Besson, L.L. Scharf, CFAR matched direction detector, IEEE Trans. Signal Process. 54 (7) (2006) 2840–2844.

[20] O. Besson, L.L. Scharf, F. Vincent, Matched direction detectors and estimators for array processing with subspace steering vector uncertainties, IEEE Trans. Signal Process. 53 (12) (2005) 4453–4463.

[21] O. Besson, Detection in the presence of surprise or undernulled interference, IEEE Signal Process. Lett. 14 (5) (2007) 352–354.

[22] A. Aubry, A.D. Maio, D. Orlando, M. Piezzo, Adaptive detection of point-like targets in the presence of homogeneous clutter and subspace interference, IEEE Signal Process. Lett. 21 (7) (2014) 848–852.

[23] F. Bandiera, O. Besson, D. Orlando, G. Ricci, L.L. Scharf, GLRT-based direction detectors in homogeneous noise and subspace interference, IEEE Trans. Signal Process. 55 (6) (2007) 2386–2394.

[24] F. Bandiera, O. Besson, G. Ricci, Direction detector for distributed targets in unknown noise and interference, Electron. Lett. 49 (1) (2013) 68–69.

[25] F. Bandiera, A. De Maio, A.S. Greco, G. Ricci, Adaptive radar detection of distributed targets in homogeneous and partially homogeneous noise plus subspace interference, IEEE Trans. Signal Process. 55 (4) (2007) 1223–1237.

[26] A. De Maio, Rao test for adaptive detection in Gaussian interference with unknown covariance matrix, IEEE Trans. Signal Process. 55 (7) (2007) 3577–3584.

[27] D. Orlando, G. Ricci, A Rao test with enhanced selectivity properties in homogeneous scenarios, IEEE Trans. Signal Process. 58 (10) (2010) 5385–5390.

[28] J. Guan, X. Zhang, Subspace detection for range and Doppler distributed targets with Rao and Wald tests, Signal Process. 91 (1) (2011) 51–60.

[29] C. Hao, D. Orlando, X. Ma, C. Hou, Persymmetric Rao, and Wald tests for partially homogeneous environment, IEEE Signal Process. Lett. 19 (9) (2012) 587–590.

[30] B. Shi, C. Hao, C. Hou, X. Ma, C. Peng, Parametric Rao test for multichannel adaptive detection of range-spread target in partially homogeneous environments, Signal Process. 108 (2015) 421–429.

[31] E. Conte, A. De Maio, Distributed target detection in compound-Gaussian noise with Rao and Wald tests, IEEE Trans. Aerosp. Electron. Syst. 39 (2) (2003) 568–582.

[32] E.J. Kelly, An adaptive detection algorithm, IEEE Trans. Aerosp. Electron. Syst. 22 (1) (1986) 115–127.

[33] F. Bandiera, M. Mancino, G. Ricci, Localization strategies for multiple point-like radar targets, IEEE Trans. Signal Process. 60 (12) (2012) 6708–6712.

[34] G.A. Fabrizio, A. Farina, M.D. Turley, Spatial adaptive subspace detection in OTH radar, IEEE Trans. Aerosp. Electron. Syst. 39 (4) (2003) 1407–1428.

[35] B. Friedlander, A subspace method for space time adaptive processing, IEEE Trans. Signal Process. 53 (1) (2005) 74–82.

[36] W. Liu, Y. Wang, W. Xie, Fisher information matrix, Rao test, and Wald test for complex-valued signals and their applications, Signal Process. 94 (2014) 1–5.

[37] J.R. Magnus, H. Neudecker, Matrix Differential Calculus with Applications in Statistics and Econometrics, Wiley, New York, NY, 2007.

[38] S.M. Kay, Fundamentals of Statistical Signal Processing: Detection Theory, Prentice-Hall, Englewood Cliffs, NJ, 1998.

[39] F. Bandiera, D. Orlando, G. Ricci, On the CFAR property of GLRT-based direction detectors, IEEE Trans. Signal Process. 55 (8) (2007) 4312–4315.

[40] K.J. Sohn, H. Li, B. Himed, Parametric GLRT for multichannel adaptive signal detection, IEEE Trans. Signal Process. 55 (11) (2007) 5351–5360.

[41] D. Sengupta, S.M. Kay, Parameter estimation and GLRT detection in colored non-Gaussian autoregressive processes, IEEE Trans. Acoust. Speech Signal Process. 38 (10) (1990) 1661–1676.

[42] F. Bandiera, O. Besson, G. Ricci, An ABORT-like detector with improved mismatched signals rejection capabilities, IEEE Trans. Signal Process. 56 (1) (2008) 14–25.